Theor Chem Acc (2000) 104:290–295
DOI 10.1007/s002140000121

Theoretical
Chemistry Accounts

Regular article

Analysis of biomolecular chaos in aqueous solution

Vincenzo Villani[1], **José M. Zaldivar Comenges**[2]

[1] Universita' della Basilicata Dipartimento di Chimica, Via N. Sauro 85, 85100 Potenza, Italy
[2] European Commission, Joint Research Center Institute for Systems, Informatics and Safety Systems Modeling and Assessment Unit, TP 250, 21020 Ispra (VA), Italy

Received: 14 September 1999 / Accepted: 3 February 2000 / Published online: 2 May 2000

Abstract. The tropoelastin peptide CH_3CO-Gly-Leu-Gly-Gly-$NHCH_3$ has been modeled in aqueous solution by means of force-field molecular dynamics simulations and its motion characterized using nonlinear dynamics theory. The trajectory $\mathbf{R}(t)$ of the representative system point in configurational space has been considered. Fractional Brownian motion with anomalous diffusion is observed resulting from chaotic dynamics of molecules on fractal media. The chaos of the peptide is a consequence of nonlinear effects such as hydrodynamic interactions of the chain due to the poor solvent role of water. The viscous drag is pointed out and should be due to the percolation network of hydrogen-bonded water molecules. The method of reconstruction of the phase space using the embedding theorem is applied to the trajectory $D_{ee}(t)$ of the peptide end-to-end distance. The existence of a low-dimensional chaotic attractor for dissipative systems has been demonstrated. The dynamical high-entropy state of the peptide in solution strengthens the transition-to-chaos mechanism for the elastin elasticity.

Key words: Molecular dynamics – CHAOS – Peptide – Elastin

1 Introduction

What is the dynamics of peptide chains in dilute aqueous solution? Of course, a simple answer is not possible: it will depend upon the particular primary structure and on the experimental conditions. Nevertheless, universal scale behavior due to the nonlinear forces is expected [1].

We will deal with the peptide CH_3CO-Gly-Leu-Gly-Gly-$NHCH_3$, with a typical sequence recurring in the tropoelastin chain. The elastin glycine-rich sequences, due to the conformational freedom and dipolar effects of this amino acid and to its distribution and high concentration in the protein (up to 33%), may characterize the elastic performance of elastin [2].

Correspondence to: V. Villani
e-mail: villani@un.bas.it

In a series of previous papers [3–7] we characterized the relative stability of conformers and the dynamical behavior of that sequence, either isolated or in solution, starting from the available experimental data [8].

Amazing nonlinear dynamical behavior with conformational solitons has been evidenced for the in vacuo molecule and chaotic behavior is suggested for the molecule in aqueous solution. In the Villani–D'Alessio–Tamburro model, this has been related to the entropic mechanism of the elastin elasticity as a chaos–soliton transition from the relaxed to the stretched form in the aqueous medium [5, 6].

The advent of nonlinear time series analysis and the mathematical theorems associated with chaotic dynamics are now making it possible not only to qualify but also to quantify the behavior of complex systems. The techniques, which consist of representing the dynamics in multidimensional phase space using delay coordinate embedding, have had success in predicting the chaotic behavior [9].

In this work, by means of force-field molecular dynamics (MD) simulations in aqueous solution and original data analysis, we are interested in investigating the complexity and instability of the nonlinear dynamics of the solvated peptide in terms of the mean squared displacement, the Hurst exponent, the fractal dimension, the attractor dimensions and Lyapunov exponents.

2 Model and methods

AMBER 4.1 software [10] was used and the data analysis was performed using self-written FORTRAN programs.

The molecular potential energy was computed using the united-atoms force field of Wiener et al. [11] for the peptide and the TIP3P model of Jorgensen et al. [12] for the water molecules.

The MD simulation at constant temperature and pressure by means of the method of Berendsen et al. [13] was accomplished by coupling the system to external heat and pressure baths at reference values $T_o = 300$ K and $P_o = 1$ atm. These dynamics are not Hamiltonian and the molecular model can be reduced to an ensemble of dissipative nonlinear Rayleigh oscillators [5, 14]. Periodic boundary conditions were applied and the cutoff distance criterion for the nonbonded interactions was used.

The equations of motion were integrated in Cartesian coordinates via the Verlet leap-frog algorithm [15] with holonomic constraints of the bond lengths at equilibrium values [16].

A solution box of density of about 1 g cm^{-3} with one CH_3CO-Gly-Leu-Gly-Gly-NCH_3 molecule solvated by 852 water molecules is the starting point of our simulation. This is the state obtained by MD simulated annealing reported in previous work [7].

In our MD simulation the integration time step was $\delta t = 1$ fs and data were stored every $\Delta t = 0.08$ ps. A time period of 1 ns was simulated, producing time series of 12,500 points.

The analysis is focused on the dynamical properties of the peptide. The trajectories $\mathbf{R}(t)$ of the representative system point in the configurational $3N$-dimensional space defined by the coordinates of each atom and $D_{ee}(t)$ of the end-to-end distance are considered. In this way, leaving the traditional partition of the molecular motion, the evolution of the whole system is analyzed. The end-to-end distance, D_{ee}, is defined by means of the end carbon atoms of acetyl and N-methyl-amide groups.

2.1 Mean squared displacement and Hurst exponent

The mean squared displacement, $\langle \mathbf{R}^2(\tau)\rangle$, is defined as the time-dependent difference correlation function [17, 18]

$$\langle \mathbf{R}^2(\tau)\rangle := \langle [\mathbf{R}(t_0) - \mathbf{R}(t_0+\tau)]^2\rangle t_0$$

at correlation times which are later by an amount τ. The time average denotes averaging over different time origins, t_0.

The scaling law of the mean squared displacement of the diffusing variable as a function of time is

$$\langle \mathbf{R}^2(\tau)\rangle \sim \tau^{2H}$$

according to the law of diffusion, where H is the critical exponent of Hurst [19–21]. We obtained the diffusion exponent, H, from the slope of the corresponding bilogarithmic scale plot:

$$\ln \langle \mathbf{R}^2(\tau)\rangle \sim 2\mathrm{H} \ln(\tau) \ .$$

When $H = 0.5$ ordinary Brownian motion occurs and the Einstein–Fick law is followed, while if $H \neq 0.5$ fractionary Brownian motion (fBm), a fingerprint of chaotic behavior, takes place [22, 23]. Both cases of enhanced and reduced diffusion speed are possible. For a random walk on a fractal object in the presence of fixed obstacles the antipersistent fBm with $H < 0.5$ occurs. In fact, the irregularities existing at all length scales are responsible for the diffusion lag [24].

2.2 Fractal dimension

How long is a dynamical path? Similarly to the Mandelbrot analysis of the coastline juggedness [25–27], the length of the trajectory $\mathbf{R}(t)$ in its multidimensional space was computed (using Euclidean metric) as a function of the resolution times $P = n\Delta t$ (n is an integer). The dimension, which is a measure of the intrinsic irregularity of the trajectory, is obtained.

In this way the lengths, $L(n)$, were measured and from the log–log plot

$$\ln [L(n)] \sim d \ln(n)$$

the corresponding fractal dimension, $D = 1 - d$, was evaluated.

2.3 Reconstructing phase space

The work of Takens [28] has shown that if the dynamics are on a d-dimensional Euclidean space, an embedding of the system can be obtained with a $2d+$ one-dimensional reconstructed state space using delay coordinates. The basic idea of this reconstruction is that if one has an orbit seen projected onto a single axis, $s(t)$, then the orbit, by virtue of the projection, overlaps with itself. If we can unfold the orbit by providing independent coordinates for a multidimensional space made out of the observations, then we can undo the overlaps coming from the projection and recover orbits which are not ambiguous.

Delay coordinates, $\{s(t),\ s(t-T),\ s(t-2T), \ldots, s[t-(d_E-1)T]\}$, are easy to work with and can be effective for very high dimensional cases. Most of the research on the state space reconstruction problem has centered on the problems of choosing the time delay, T, and the embedding dimension, d_E, for delay coordinates.

2.4 Finding the time delay

The first step in phase-space reconstruction is to choose an optimum lag parameter, T. The most useful technique was suggested by Fraser and Swinney [29]. They propose using the first minimum of the average mutual information function, $I(T)$, as a kind of nonlinear correlation function. At this time, the values of $s(t)$ and $s(t-T)$ are independent enough of each other to be useful as coordinates in a time delay vector.

2.5 Choosing the embedding dimension

The time delay reconstruction of the system phase space provides the necessary number of coordinates to unfold the attractor called the embedding dimension, d_E [30].

We used the Cao method [31], which is based on the idea of false nearest neighbors (FNN) developed by Kennel et al. [32]. In this case, the condition of no self-intersection states that if the attractor is to be reconstructed successfully in R^d, then all the neighboring points in R^d should also be neighbors in R^{d+1}. This d is chosen as the embedding dimension. This method also provides a way to distinguish between deterministic and stochastic signals by plotting two functions E1 and E2 (see Cao [31] for the precise definition). When both quantities reach the saturation we find the embedding dimension. In case of noise, E1 will never reach the saturation and E2 will always remain unity for any dimension.

2.6 Determining the dynamical dimension

Once one has determined the global number of dimensions required to unfold the attractor, there remains the problem of the number of dynamical degrees of freedom, d_L, which are active in determining the evolution of the system as it moves around the attractor [32]. To calculate this dynamical dimension we used the method proposed by Kennel et al. [33], which consists in evaluating the percentage of local FNNs. Using the same idea as the method of FNNs, they proposed a method to study the local structure of the phase space to see if locally one requires fewer dimensions than d_E to capture the evolution of the orbits as they move on the attractor. Their approach was to work in a dimension, $d \geq d_E$, large enough to assure that the attractor has been unfolded. In this space, they studied for some data point $y(k) = \{s(t),\ s(t-T),\ s(t-2T), \ldots, s[t-(d-1)T]\}$ what subspace of dimension $d_L \leq d_E$ allows accurate local neighborhood-to-neighborhood maps of the data on the attractor to be made. In fact, for a specified number of neighbors, N_B, of $y(k)$, they provided a local rule for calculating how these points evolve in one time step into the same N_B points near $y(k+1)$. When the percentage of bad predictions becomes independent of d_L and is also insensitive to N_B, it is possible to say that the correct local dimension for the active degrees of freedom has been identified.

2.7 Global Lyapunov Exponents

Given a dynamical system in a d-dimensional phase space it is possible to monitor the evolution of an infinitesimal d-sphere of initial conditions. This d-sphere will become a d-ellipsoid due to the locally deforming nature of the flow. The jth one-dimensional Lyapunov exponent, λ_j, is then defined in terms of the length of the ellipsoidal principal axes, $p_j(t)$, at time t as [34]

$$\lambda_j = \lim_{t\to\infty} 1/t \log_2 p_j(t)/p_j(0), \quad j = 1, \ldots, d_L$$

The Lyapunov exponent monitors the behavior of two closely neighboring points in a direction of the phase space as a function of time. If the points expand away from each other, the Lyapunov

exponent will be positive, if they converge, the exponent becomes negative and if the two points stay the same distance apart, the exponent stays near zero. If base 2 is used, the exponents are measured in bits of information per time unit.

3 Results and discussion

3.1 Scaling law and fractal dimension

The bilogarithmic scale plot of the length $L(n)$ of the trajectory $\mathbf{R}(t)$ as a function of the resolution factor n per measurement interval is reported in Fig. 1. The asymptotic straight behavior has been fitted by the least-squares regression line.

The computed critical exponent, increasing the trajectory length, is $d = 0.71$. As far as the fractal dimension $D = 1.71$ is concerned we observe that it is larger than that corresponding to ideal Brownian walks ($D = 1.5$) and that it is typical of antipersistent fBm related to critical self-organized phenomena [35]. This motion has a lower correlation time than a Brownian one, with a greater entropy and is a fingerprint of chaotic dynamics.

These observations confirm the previous hypotheses [5, 6] of the great change in solution of the dynamical picture with respect to the in vacuo molecule characterized by soliton vibrations.

3.2 Mean squared displacement and Hurst exponent

The log–log plot of the time-dependent mean squared displacement, $\langle \mathbf{R}^2(\tau) \rangle$, versus the correlation time, τ, is reported in Fig. 2. In the meaningful time range, not affected by the finite length of the series, the function has a linear behavior and it is possible to evaluate the Hurst exponent $H = 0.30$. The observed value is lower than that corresponding to ideal Brownian walks ($H = 0.5$), pointing to a reduced diffusion and consistent with the value of the observed fractal dimension of $\mathbf{R}(t)$.

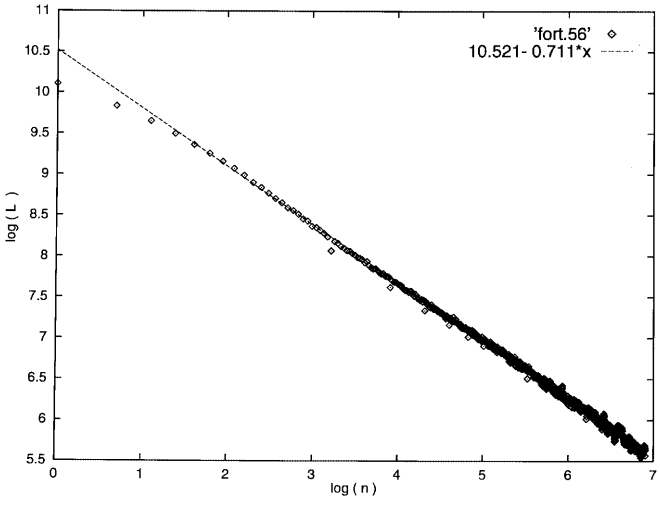

Fig. 1. Log–log plot of the measured length, $L(n)$, for the trajectory $\mathbf{R}(t)$ as a function of the resolution factor, n, per observation period

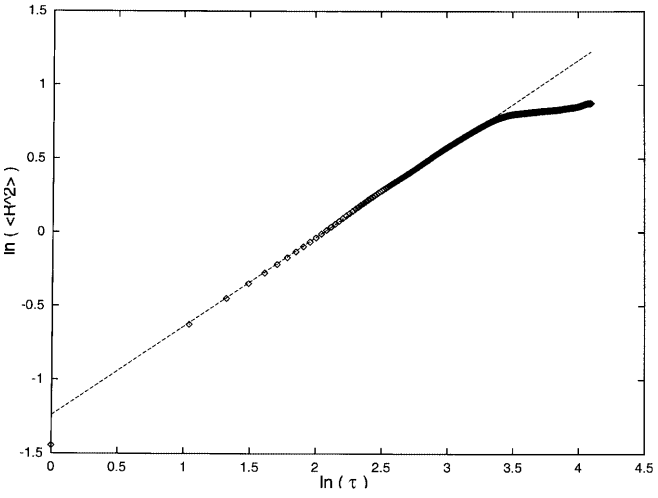

Fig. 2. Log–log plot of the mean squared displacement, $\langle \mathbf{R}^2(\tau) \rangle$, versus the autocorrelation time, τ. The displacement is expressed in angstroms and the time unit in 0.08 ps

The anomalous diffusion is in agreement with the antipersistent fBm of molecules in fractal media. From this point of view, we hypothesize that the diffusion lag is due to the viscous drag of the solution hydrogen-bonded network. In other words, the hydrogen-bonded water molecules make a percolation cluster of obstacles against the solute motion, and similarly to the findings of simple lattice models deviation from ideal diffusion is observed.

Let us remember that a great correspondence does exist between the scaling laws of the chain size as a function of the chain length, N, or the time period, τ. The former is characterized by the Flory critical exponent [1], ν, the later by the Hurst one. From this viewpoint, these exponents can be interpreted in the same way. Then, the observed H value is in agreement with $\nu = 1/3$ expected in poor solvents [1], where the solute–solvent interactions are unfavored with respect to the intramolecular ones within the solute, because of the poor hydrophilicity of the peptide.

In conclusion, the dynamics of the elastin tetrapeptide in aqueous solution could be modeled by means of chaotic motion in fractal percolation media of hydrogen-bonded water molecules.

3.3 Attractor dimensions and Lyapunov exponents

To analyze the chaos quantitatively the Lyapunov exponents of the trajectory $D_{ee}(t)$ for the peptide end-to-end distance were considered.

The time series data of $D_{ee}(t)$ were used to calculate the $I(T)$ function. The first minimum of the average mutual information function occurs at $T = 17\Delta t$ (1.36 ps).

Using the time lag $T = 16\Delta t$ and $17\Delta t$, the functions E1 and E2 were calculated. As can be seen in Fig. 3, the saturation is reached at $d_E \sim 11$ after which it remains approximately constant. This provides evidence that we are dealing with a low-dimensional system.

For the $D_{ee}(t)$ trajectory the percentage of bad predictions seen in Fig. 4 becomes independent of the number of neighbours, N_B, and of the local dimension at $d_L \sim 9$, telling us that this attractor may be adequately described by nine degrees of freedom. This means that models for simulating the dynamic behavior of this peptide should have local nine-dimensional dynamics regardless of the dimensions of the overall space in which the model is built.

These results shed light on the amazing chance of performing simulations only along the few active dynamical degrees of freedom. By reducing drastically the dimension of the conformational phase space for dispersed molecules in solution, it would be possible to perform long-time force-field simulations, characterizing slow molecular motions, such as helix–coil transitions and protein folding in biopolymers, or reptation in non biological polymers, which are at present not possible to investigate and are unlikely to be treatable for many years [36]. In this framework Amadei and coworkers [37–39] have developed the essential dynamics method. This approximation is linear and therefore can be improved. Nevertheless, the analysis outcome using chaos techniques confirms it.

The nine computed local Lyapunov exponents forwards and backwards in time are shown in Fig. 5. As

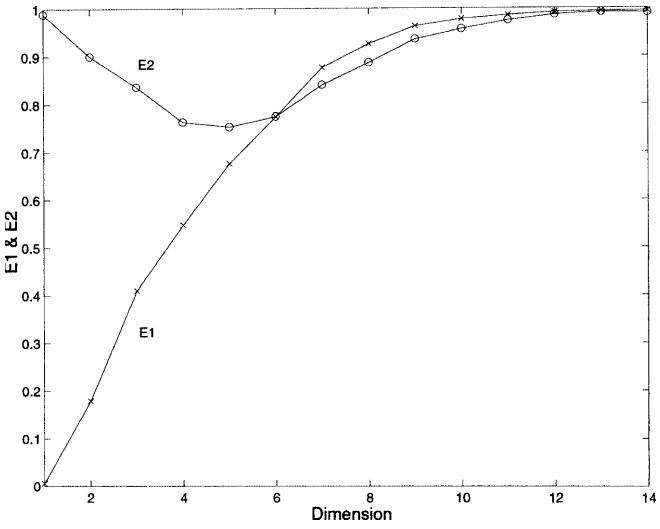

Fig. 3. Values of E1 and E2 functions (see text) for the end-to-end distance trajectory $D_{ee}(t)$

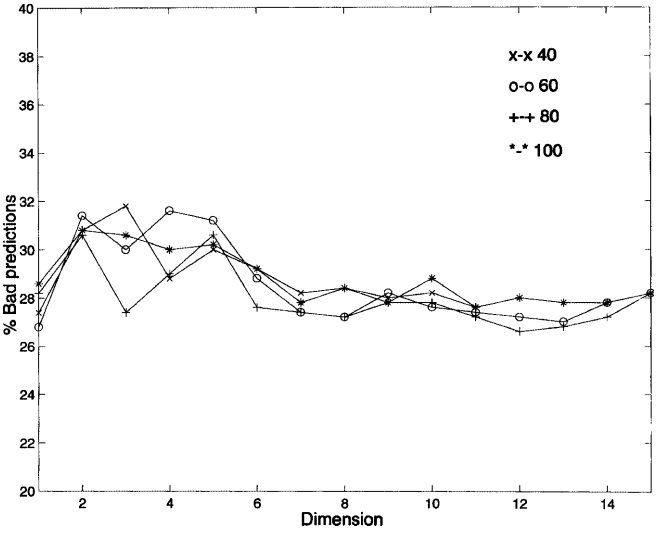

Fig. 4. Percentage of local false nearest neighbors as a function of the embedding dimension for the end-to-end trajectory $D_{ee}(t)$. $N_B = 40$, 60, 80 and 100 neighbors are considered. From this view $d_L \sim 9$ might be chosen. Recall $d_E \sim 11$

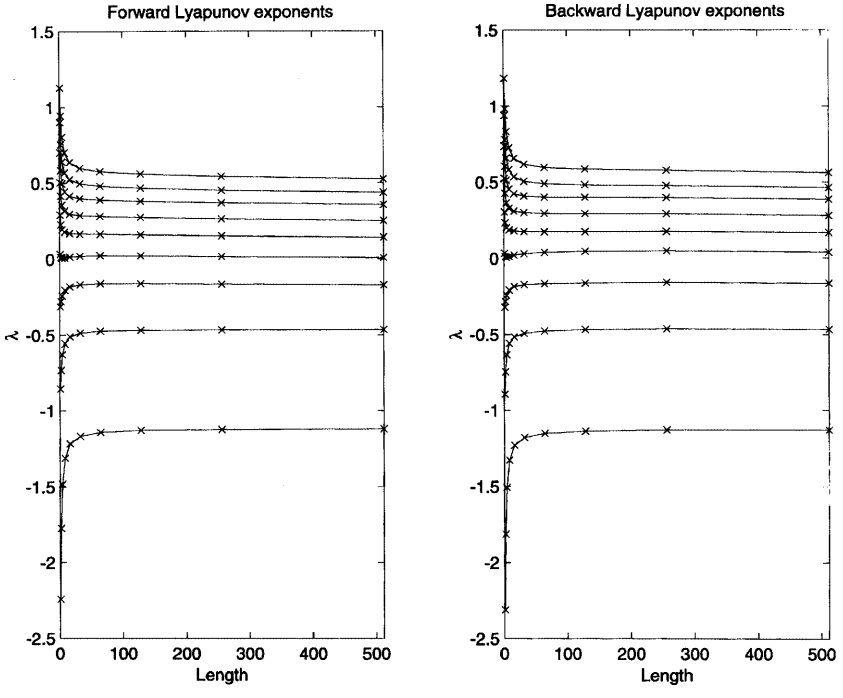

Fig. 5. Average local Lyapunov exponents, λ, for the end-to-end distance trajectory $D_{ee}(t)$ computed forwards and backwards in time using $d_L = 9$. The length is expressed in 2^{L-1} where L is the number of time steps away from the time of perturbation. λ is in units of 12.5 ps^{-1}. For large L local exponents become global (they converge to stable values)

Table 1. Lyapunov exponents, λ, of Fig. 5 for $D_{ee}(t)$, computed forwards and backwards in time, are summarized. Also the total sum is reported

λ_j	End-to-end distance		x-Coordinate	
	Forward	Backward	Forward	Backward
1	0.5244	0.5617	0.5268	0.5425
2	0.4376	0.4644	0.4356	0.4534
3	0.3556	0.3870	0.3487	0.3673
4	0.2519	0.2810	0.2564	0.2734
5	0.1425	0.1684	0.1378	0.1509
6	0.0082	0.0402	−0.0057	0.0141
7	−0.1734	−0.1656	−0.2039	−0.1762
8	−0.4646	−0.4669	−0.4887	−0.4426
9	−1.1203	−1.1277	−1.1059	−1.1359
Sum	−0.0380	0.1426	−0.0988	0.0470

can be seen, five Lyapunov exponents are positive, one is close to zero and the others are negative. The results are summarized in Table 1, which also gives a negative total sum of the Lyapunov exponents, as expected for a dissipative system. As can be seen, the computation of the Lyapunov exponents forwards and backwards in time gives approximately the same results, which tell us that the dynamical dimension has been correctly calculated.

The existence of positive Lyapunov exponents demonstrates further and strictly the chaos of peptide dynamics. The chaotic behavior of the tetrapeptide in solution, already hypothesized by one of us [5, 6], plays a fundamental role in the expression of the restoring force in the entropic mechanism of elastin elasticity. Our findings are in agreement with the experimental evidence of Gaspard et al. [40] for microscopic chaos in fluid systems obtained by the observation of Brownian motion of a colloidal particle suspended in water. Moreover, they are in the framework of the chaotic hypotheses of Krylov [41] (who referred to microscopic dynamical instabilities) and Gallavotti and Cohen [42], which suppose that the properties of statistical mechanics can be predicted by treating the systems as chaotic.

4 Conclusions

The configurational trajectory $\mathbf{R}(t)$ of the elastin peptide in aqueous solution was analyzed and its fractal dimension ($D = 1.71$) and the anomalous diffusion of its motion ($H = 0.30$) were determined. The observed behavior departs from the ideal Brownian motion because of the nonlinear interactions in solution, such as hydrodynamic interactions [43] (i.e. the fluctuating force on any chain unit turns out to be correlated with the force on other distant ones) and the hydrogen-bonded network. It is close to the random walks of chains in poor solvents characterized by the Flory exponent $\nu = 1/3$. The observed anomalous diffusion is coherent with the fractional Brownian motion in fractal media: the diffusion lag could be due to the percolation cluster of the solution hydrogen-bonded network.

The trajectory $D_{ee}(t)$ of the end-to-end distance was analyzed using delay coordinate embedding in an effort to understand the nonlinear dynamic behavior of the system. The analysis using the standard time delay embedding techniques seems to indicate low-dimensional chaotic dynamics ($d_E = 11$, $d_L = 9$ and five positive Lyapunov exponents). Even though the original system has a large number of degrees of freedom, the results seem to indicate that only a few degrees of freedom are active in the final attractor and that the dynamics of such a system could be described by a reduced number of differential equations.

The existence of a low-dimensional chaotic attractor with few dynamical degrees of freedom active in determining the evolution of the system is typical of nonlinear dissipative systems [44], to which molecules in solutions belong, and is consistent with the Langevin dynamics description [45]. Similar results have been obtained by one us concerning the folding of a small protein simulated as a Langevin system [46] or by Zhou and Wang on a polyalanine peptide [47].

Chaos is a sufficient but not necessary condition for Brownian motions [48]. In fact, the analysis of simplified models showed that the erratic motion of dispersed particles can be due largely to the randomness of the initial conditions of the fluid molecules [49]. Chaos is defined mathematically in terms of positive Lyapunov exponents. In this way we showed that the conformational motion of the elastin peptide in aqueous solution has chaotic dynamics after all.

The collective dynamics of the oligopeptide of the tropoelastin chain floating in dilute solution is inherently nonlinear and chaotic behavior is observed. In elastin further nonlinear effects fundamental to the peculiar macroscopic properties of the protein have to be taken into account. The most important is certainly that due to desmosine and isodesmosine cross-links recurring up to about 30 amino acids [50], which reticulate tropoelastin chains forming the elastin elastic percolation network [51, 52].

We suggest that the physical behavior of elastin is a consequence of its nonlinear effects developed at the protein–water interface, where glycine-rich chain portions, similar to the sequence of our peptide, are likely to be located and chaotic dynamics are expected.

References

1. de Gennes PG (1979) Scaling concepts in polymer physics. Cornell University Press, Ithaca
2. Tamburro AM (1990) In: Tamburro AM, Davidson JM (eds) Elastin: chemical and biological aspects. Congedo, Italy, p 126
3. Villani V, Tamburro AM (1993) J Chem Soc Perkin Trans 2: 1951
4. Villani V, Tamburro AM (1995) J Biomol Struct Dyn 12: 1173
5. Villani V, D'Alessio L, Tamburro AM (1997) J Chem Soc Perkin Trans 2: 2375
6. Villani V, D'Alessio L, Tamburro AM (1997) In: Tamburro AM (ed) Elastin and elastic tissue. Armento, Potenza, Italy, p 31
7. Villani V, Tamburro AM (1998) J Mol Struct (Theochem) 431: 205

8. Tamburro AM, Guantieri V, Pandolfo L, Scopa A (1990) Biopolymers 29: 855
9. Abarbanel HDI (1996) Analysis of observed chaotic data. Springer, Berlin Heidelberg New York
10. Pearlman DA, Case DA, Caldwell JC, Ross WS, Cheatham TE III, Ferguson DM, Seibel GL, Chandra Singh U, Weiner P, Kollman PA (1995) AMBER 4.1 University of California, San Francisco
11. Weiner SJ, Kollman PA, Nguyen DT, Case DA (1986) J Comput Chem 7: 230
12. Jorgensen WL, Chandrasekhar J, Madura JD, Impey RW, Klein ML (1983) J Chem Phys 79: 926
13. Berendsen HJC, Postma JPM, van Gunsteren WF, Di Nola A, Haak JR (1984) J Chem Phys 81: 3684
14. Hoover WG (1985) Phys Rev A 31: 3
15. Verlet L (1967) Phys Rev 98: 159
16. Ryckaert JP, Ciccotti G, Berendsen HJC (1977) J Comput Phys 23: 327
17. Bunde A, Havlin S (1992) Fractals and disordered systems. Springer Berlin Heidelberg New York
18. Schoen M (1993) Computer simulation of condensed phase in complex geometries. Springer, Berlin Heidelberg New York
19. Hurst HE (1951) Trans Am Soc Civ Eng 116: 770
20. Feder J (1988) Fractals Plenum, New York
21. Cannon et al (1997) Physica A 241: 606
22. Mandelbrot BB, Van Ness JW (1968) SIAM Rev 10: 422
23. Mandelbrot BB (1982) The fractal geometry of nature. Freeman, New York
24. Metzler R, Glockle UG, Nonnenmacher TF (1994) Physica A 211: 13
25. Mandelbrot BB (1967) Science 155: 636
26. Mandelbrot BB (1975) Proc Natl Acad Sci USA 72: 3825
27. Mandelbrot BB (1977) Fractals: form, chance, and dimension. Freeman, San Francisco
28. Takens F (1981) In: Rand A, Young LS (eds) Lecture notes in mathematics vol 898. Springer, Berlin Heidelberg NewYork, p 366
29. Fraser A, Swinney H (1986) Phys Rev A 33: 1134
30. Grassberger P, Procaccia I (1983) Phys Rev Lett 50: 346
31. Cao L (1997) Physica D 110: 43
32. Kennel MB, Brown R, Abarbanel HDI (1992) Phys Rev A 45: 3403
33. Kaplan JL, Yorke JA (1979) In: Peitgen HO, Walther HO (eds) Functional differential equations and approximation of fixed points. Springer, Berlin Heidelberg NewYork, pp 204–227
34. Wolf A, Swift JB, Swinney HR, Vastan JA (1985) Physica D 16: 285
35. Bak P, Tang K, Wiesenfeld K (1987) Phys Rev Lett 59: 381
36. Chan HS, Dill KA (1993) Physics Today 46: February 24
37. Amadei A, Linssen A, Berendsen JC (1993) Proteins Struct Funct Genet 17: 412
38. Amadei A et al (1996) J Biomol Struct Dyn 13: 615
39. Van Aalten et al (1997) J Comput Chem 18: 169
40. Gaspard P, Briggs ME, Francis MK, Sengers JV, Gammon RW, Dorfman JR, Calabrese RV (1998) Nature 394: 865
41. Krylov N (1944) Nature 153: 709
42. Gallavotti G, Cohen EGD (1995) Phys Rev Lett 74: 2694
43. Zwanzig R (1969) In: Shuler KE (ed) Advances in chemical physics, vol. XV. Stochastic processes in chemical physics. Wiley New York, p 325
44. Schuster HG (1995) Deterministic chaos. VCH, Weinheim
45. van Gunsteren WF, Berendsen HJC, Rullmann JAC (1981) Mol Phys 44: 69
46. Zaldivar JM, Abecasis A (1999) 5th SIAM Conference on Dynamical Systems, Snowbird, Utah, USA, 25–27 May 1999
47. Zhou H, Wang L (1996) J Phys Chem 100: 8101
48. Durr D, Spohn H (1998) Nature 394: 831
49. Spohn H (1991) Large scale dynamics of interacting particles. Springer, Berlin Heidelberg New York
50. Thomas J, Elsden DF, Partridge SM (1963) Nature 200: 651
51. Sahimi M (1994) Applications of percolation theory. Taylor & Francis, London
52. Bastide J, Boue F (1986) Physica A 140: 251